ISSN PRINT 2319 1775 Online 2320 7876

Research paper UGC CARE Listed (Group -I) Journal Volume 10, Iss 3, 2021

GPS Data and SHF Modelling of the Low-Latitude Ionosphere

D. Venkata Ratnam

Department of ECE, Koneru Lakshmaiah Education Foundation, Green Fields, Vaddeswaram, Andhra Pradesh 522 502, India.

Abstract

The model is based on spherical harmonic functions (SHF), which provide a suitable representation for ionospheric behavior. The model is constructed by computing spherical harmonic coefficients through a weighted least square method, utilizing measured vertical total electron content (TEC) data from seventeen GPS Aided Geo Augmented Navigation stations.The accuracy of the SHF model is evaluated based on the residual error and compared with other standard grid models. The diurnal TEC variations are well represented by the SHF model, and it also demonstrates good performance in depicting ionospheric delays during the summer and autumn equinox seasons. Overall, the results indicate that the SHF model is effective in estimating ionospheric delays and provides valuable insights into ionospheric behavior in the Indian region.

INTRODUCTION

This paper focuses on ionospheric modeling for GPS Aided Geo Augmented Navigation (GAGAN) in the Indian region, which is prone to significant ionospheric delay variations due to its location in the equatorial anomaly region. A spherical harmonic function (SHF) model is implemented using data from 17 GPS stations in India to estimate ionospheric grid point (IGP) delays [1]. The SHF model provides information about the horizontal characteristics of the ionosphere. The SHF model represents the horizontal ionospheric profile as a Fourier series expansion in terms of ionospheric pierce point (IPP) longitudes and latitudes [2]. The IPP is the intersection point of the line of sight from a receiver to a GPS satellite and an imaginary shell defined at a designated height of 350 km. The SHF model is based on solutions to Laplace's equations and represented in spherical coordinate system. The paper discusses the maximum, mean, and standard deviation of ionospheric delays at various IGP locations over several months [3-5]. Additionally, it compares the SHF ionospheric delay model with other models such as minimum mean square error (mmse), planar fit model (PFM), kriging

ISSN PRINT 2319 1775 Online 2320 7876

Research paper UGC CARE Listed (Group -I) Journal Volume 10, Iss 3, 2021

technique, and inverse distance weight (IDW) for both quiet and disturbed days at a typical IGP location (25° N, 75° E) [6].

II.SHF ALGORITHM

The SHF algorithm is used for modeling the ionospheric delays in the GPS Aided Geo Augmented Navigation (GAGAN) system. It is based on spherical harmonic functions, which are a set of orthogonal solutions to Laplace's equations in a spherical coordinate system. The algorithm utilizes data from 17 GPS stations over the Indian region to estimate ionospheric grid point (IGP) delays [7]. The SHF model represents the horizontal characteristics of the ionosphere by employing a Fourier series expansion in terms of ionospheric pierce point (IPP) longitudes and latitudes. The IPP is the point where the line of sight from a receiver to a GPS satellite intersects with an imaginary shell at a specified height of 350 km.Using the measured vertical total electron content (TEC) data and basis functions, the SHF algorithm computes the spherical harmonic coefficients through a weighted least square method. These coefficients are then used to model the ionospheric delays at different grid points [8-10]. The paper presents the results of the SHF model in terms of accuracy, residual errors, and diurnal TEC variations. It also compares the performance of the SHF model with other standard grid models, such as minimum mean square error (mmse), planar fit model (PFM), kriging technique, and inverse distance weight (IDW), for both quiet and disturbed days at a typical IGP location (25° N, 75° E).Overall, the SHF algorithm proves to be capable of estimating ionospheric delays effectively, making it a valuable tool for ionospheric modeling in the GAGAN system [11-13].

ISSN PRINT 2319 1775 Online 2320 7876

Research paper UGC CARE Listed (Group -I) Journal Volume 10, Iss 3, 2021

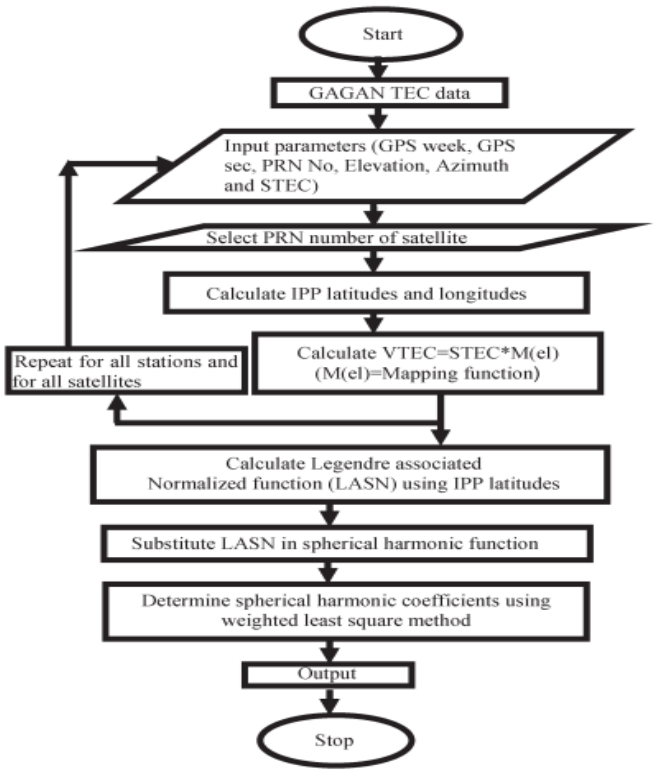

Fig. 1. Flow chart for computing the spherical harmonic coefficients.

IV. RESULTS AND DISCUSSION

A. Analysis of One Epoch Data

The data from a typical epoch [14.00 local time (LT) of July 25, 2004] are taken into account in the analysis. 13.4 m is the highest TEC value. The VTEC values are computed using spherical harmonic coefficients, and the maximum TEC is 11.4 m (Fig. 4). These graphs clearly show that the measured and calculated TEC values closely track one another. By contrasting the residuals, the performance accuracy of the spherical harmonics is evaluated. The predicted TEC is subtracted from the measured TEC data (IPP vertical delays) to determine the residuals.

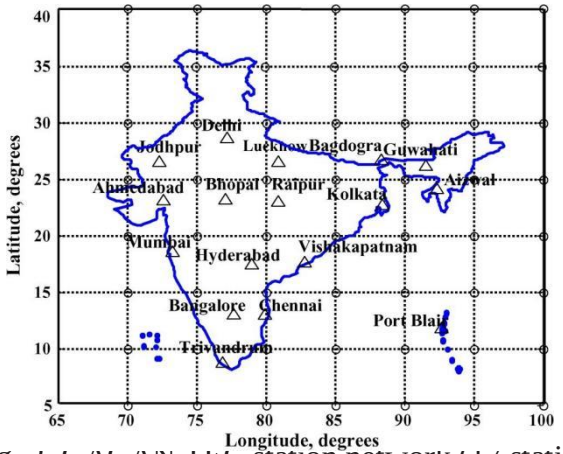

Fig. 2. GAGAN TEC station network (17 stations are indicated).

ISSN PRINT 2319 1775 Online 2320 7876

Research paper UGC CARE Listed (Group -I) Journal Volume 10, Iss 3, 2021

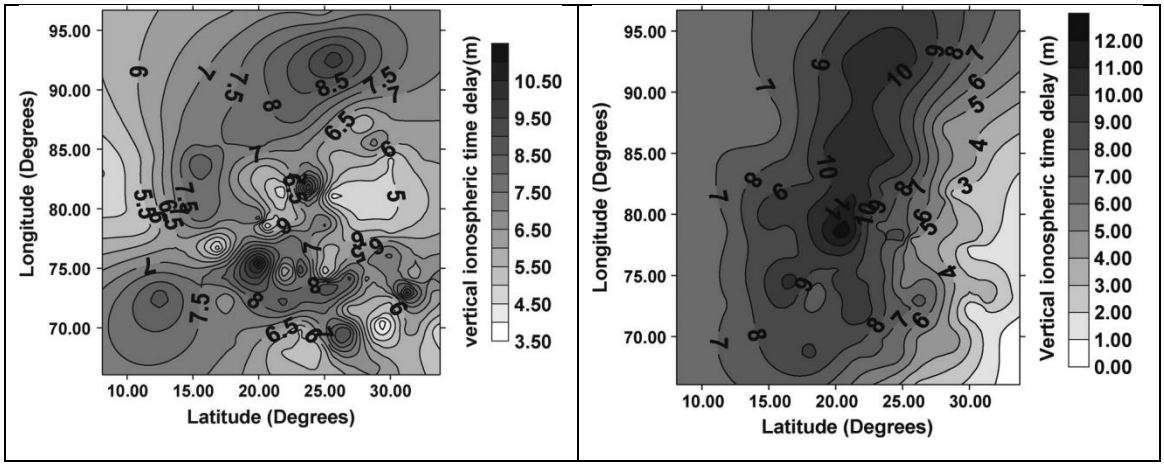

Fig. 4. Estimated TEC values on July 25, 2004, at 14.00 h (LT). Fig. 3. Measured TEC values on July 25, 2004, at 14.00 h (LT).

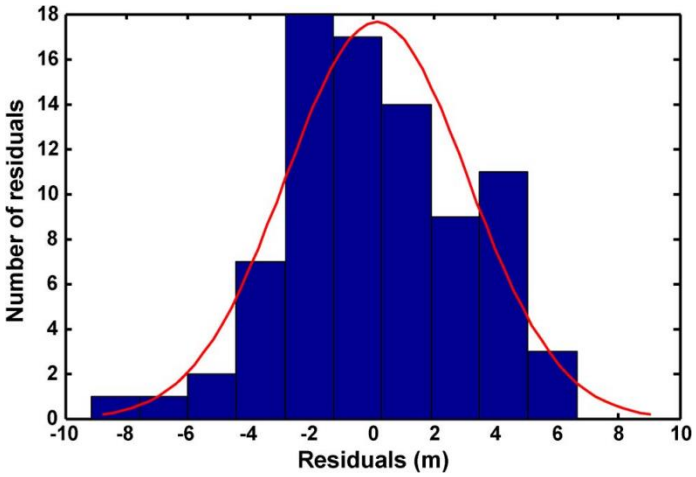

Fig. 5. Distribution of residuals due to the SHF model [July 25, 2004, at 14.00 h (LT)].

Over the New Delhi airport (28.58 N, 77.21 E), IGP delay variations are examined for both calm and turbulent days (July 5 and 25, 2004). For evaluating their delays, the four adjacent IGPs (25 N, 75 E, 30 N, 75 E, 25 N, 80 E, and 30 N, 80 E) are taken into account. The greatest Kp index.whereas it is eight on a disturbed day, value is two on a tranquil day. The Ap index values are 2 for the tranquil day and 194 for the disturbed day. The maximum TEC in a day, along with the global Kp and Ap indices, are used to determine whether days have magnetically quiet and disturbed ionospheric conditions. A three-hourly planetary geomagnetic measure of activity collected from 12 or 13 sites spread out throughout the globe is known as the Kp index.

ISSN PRINT 2319 1775 Online 2320 7876

Research paper UGC CARE Listed (Group -I) Journal Volume 10, Iss 3, 2021

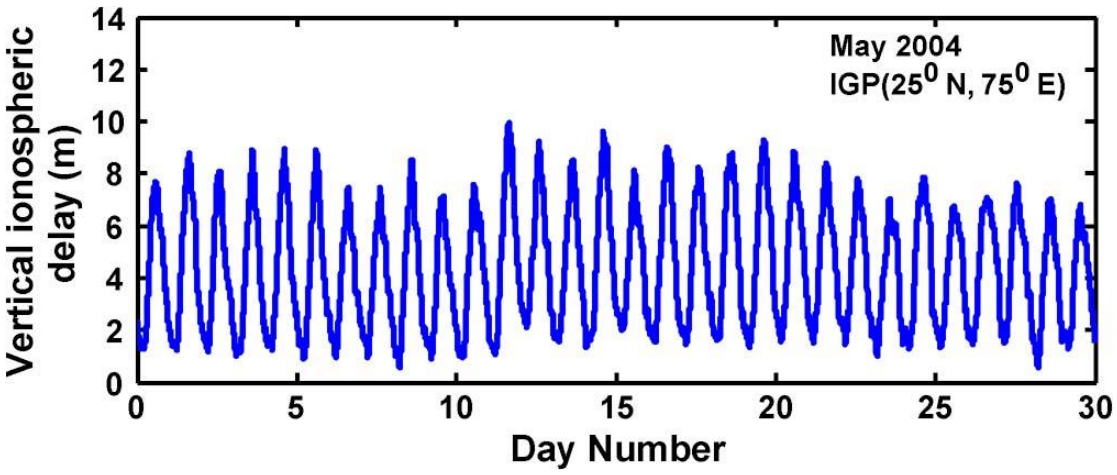

Fig. 8. IGP delay variations for May 2004.

The study includes estimations of IGP delays for 24 hours over the Indian region, along with the identification of maximum and minimum delay values and their corresponding locations (Table II). The results indicate that the maximum IGP delay varies from 5.25 to 6.17 meters, while the minimum IGP delay varies from 0.66 to 1.78 meters. It is noteworthy that the maximum peak delays tend to occur during the time interval of 12:16 to 16:00 hours on a quiet day.For the analysis of disturbed day data (July 25, 2004), Table III presents the maximum and minimum IGP delays along with their corresponding times. Figure 7 displays the variations in IGP delays for the disturbed day. The maximum ionospheric delay is observed to be 8.1 meters at 16:08 hours, while the minimum ionospheric delay is 1.33 meters at 3:92 hours. The results clearly demonstrate that the IGP delay values are higher during disturbed days compared to quiet days. This phenomenon is attributed to the impact of magnetic storms on the equatorial anomaly, leading to rapid penetration of electric fields into the mid and equatorial ionosphere. As a result, maximum delays are more likely to occur during these times.

Estimation of the Monthly IGP Delay, C

The predicted monthly IGP delays are used to study the daily ionospheric variability. These six-month analysis data, from May, June, July, August, September, and October 2004, are taken into consideration. Figs. 8–19 exhibit the monthly fluctuations in ionospheric delay. Ionospheric delays are calculated for the month of May 2004 at an IGP (25 N, 75 E), which is situated close to the northern equatorial anomaly crest zone, using the SHF model.

ISSN PRINT 2319 1775 Online 2320 7876

Research paper UGC CARE Listed (Group -I) Journal Volume 10, Iss 3, 2021

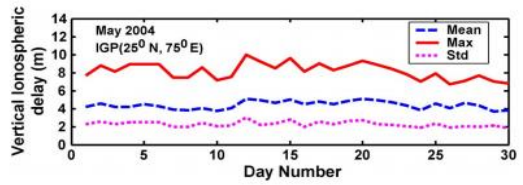

Fig. 9. Daily mean, maximum, and standard deviation of IGP delay variations for May 2004.

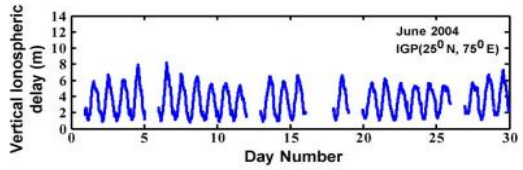

Fig. 10. IGP delay variations for June 2004.

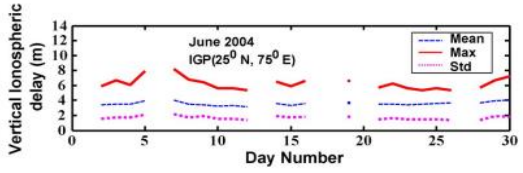

Fig. 11. Daily mean, maximum, and standard deviation of IGP delay variations for June 2004.

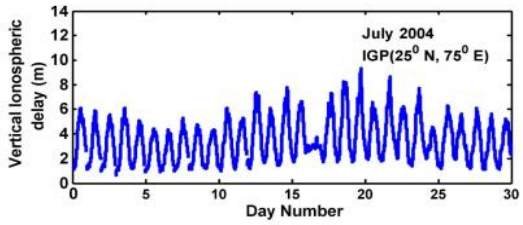

Fig. 12. IGP delay variations for July 2004.

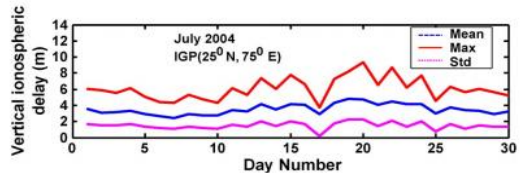

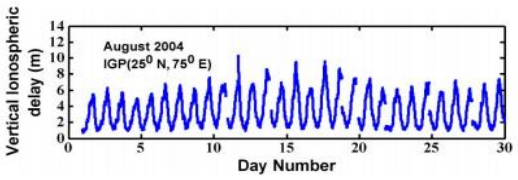

Fig. 14. IGP delay variations for August 2004.

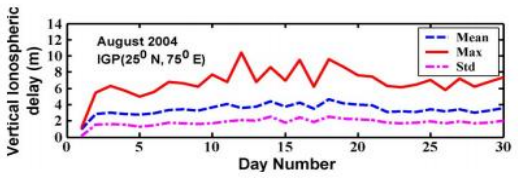

Fig. 15. Daily mean, maximum, and standard deviation of IGP delay variations for August 2004.

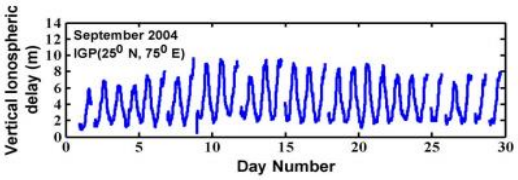

Fig. 16. IGP delay variations for September 2004.

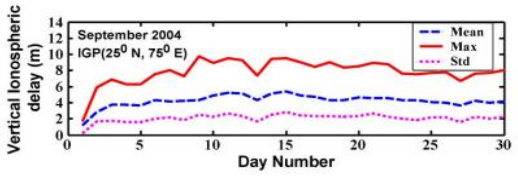

Fig. 17. Daily mean, maximum, and standard deviation of IGP delay variations for September 2004.

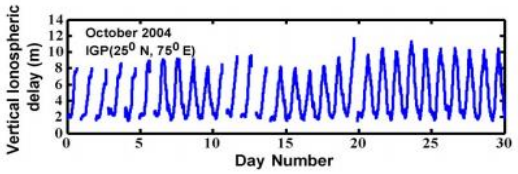

Fig. 18. IGP delay variations for October 2004.

In Fig. 8, the IGP delay values are displayed. The image clearly illustrates the ionosphere's diurnal behaviour for a period of 30 days. On May 12, 2004, the maximum IGP delay is 9.96 m. Additionally calculated (Fig. 9) are the daily maximum, mean, and standard deviation of IGP delays.The greatest values of the mean and standard deviation of the ionospheric delay were 5.1 and 3.03 m, respectively.2) For the month of June 2004, IGP (25 N, 75 E) delays are projected (Fig. 10). On June 7, 2004, the highest delay (8.20 m) takes place. Seven days of the data for this month—days 1, 6, 13, 17, 18, 20, and day 28—are not accessible.

ISSN PRINT 2319 1775 Online 2320 7876

Research paper UGC CARE Listed (Group -I) Journal Volume 10, Iss 3, 2021

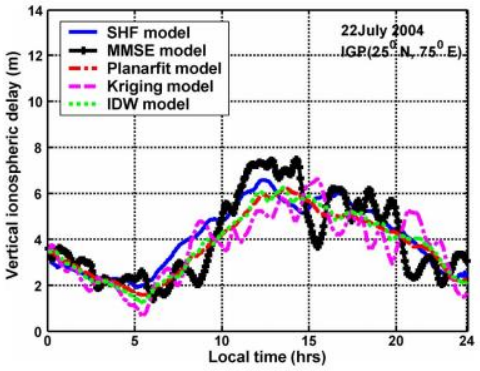

Fig. 22. Comparison of the SHF model with other models for a typical quiet day.

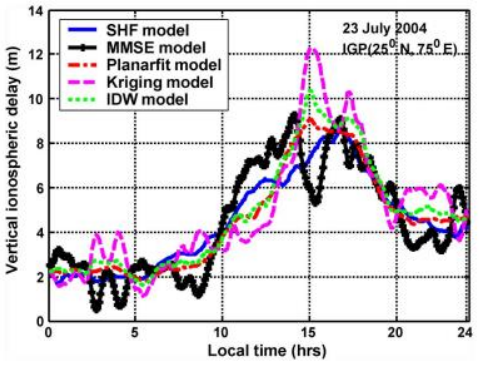

Fig. 23. Comparison of the SHF model with other models for a typical disturbed day.

Ionospheric grid models had respective heights of 6.19, 6.59, 6.23, and 7.49 m (Fig. 22). All five models' results are found to follow the same half-cosine pattern, which exhibits diurnal fluctuations in ionospheric delays. Table IV displays the maximum, mean, and standard deviation of the ionospheric delays for each model. The five models' standard deviations are found to be between 1.38 and 1.80 m. The term "difference" refers to the variation in ionospheric delays between the SHF model and other models. Table V displays the maximum, mean, and standard deviation of the differences.The maximum (1.19 m) and standard deviation (0.49 m) of the SHF and PFM models are lower than those of other models (Table V).

CONCLUSION

On a calm day, the highest ionospheric delay was recorded at IGP (25 N, 85 E) at 14.25 h, while in IGP (30 N, 80 E) at 16.08 h on a disturbed day, the maximum ionospheric delay was recorded at 6.17 m. It has been noted that IGP delays are higher around the autumnal equinox than they are in the summer. Other common models are contrasted with the SHF model. It is located Thus for both disturbed and calm days, the difference in the standard deviations between SHF and PFM models is smaller and they closely follow one another. Therefore, satellite-based navigation systems can also take into account the SHF model. Investigating ionospheric properties would benefit from the assessment of monthly and seasonal ionospheric delay fluctuations. Since the data used in this study are only from a small area, it may be

ISSN PRINT 2319 1775 Online 2320 7876

Research paper UGC CARE Listed (Group -I) Journal Volume 10, Iss 3, 2021

possible to improve accuracy by using spherical cap harmonic and modified spherical harmonic approaches.

REFERENCES

1. D. L. Opperman, "Reconstructing ionospheric TEC over South Africa using signals from a regional GPS network," Ph.D. dissertation, Rhodes Univ., Grahamstown, South Africa, Nov. 2007.
2. M. J. Mohlenkamp. (2010). A User's Guide to Spherical Harmonics.[Online]. Available: http://www.ohio.edu/people/mohlenka/research/uguide.pdf
3. A. D. Sarma, N. Prasad, and T. Madhu, "Investigation of suitability of grid-based ionospheric models for GAGAN," Electron. Lett., vol. 42,no. 8, pp. 478–479, Apr. 2006.
4. A. Vallado, Fundamentals of Astrodynamics and Application.New York: McGraw-Hill, 1997, ser. Space Technology Series.
5. S. Schaer, G. Beutler, M. Rothacher, and T. A. Springer, "Daily global ionosphere maps based on GPS carrier phase data routinely produced bythe code analysis center," in Proc. IGS AC Workshop, Silver Spring, MD,Mar. 19–21, 1996.
6. J. Hopkins, "Computation of normalized associated Legendre functions using recursive relations," J. Geophys. Res., vol. 78, no. 2, pp. 476–477,1973.
7. R. Langley, M. Fedrizzi, E. Paula, M. Santos, and A. Komjathy, "Mapping the low latitude ionosphere with GPS," GPS World, vol. 13, no. 2, pp. 41–46, 2002.
8. S. Basu and S. Basu, "Effects of large magnetic storms on communication and GPS navigation systems at middle and equatorial latitudes," in Proc.URSI GA Int. Conf., Maastricht, The Netherlands, Aug. 17–24, 2002.
9. H. Rishbeth and C. S. G. K. Setty, "The F-layer at sunrise," J. Atmos.Terr. Phys. (UK), vol. 20, no. 4, pp. 263–276, Apr. 1961.
10. J. Blanch, T. Walter, and P. Enge, "Adapting kriging to the WAAS MOPS ionospheric grid," in Proc. NTM Inst. Navig., Anaheim, CA, Jan. 2003,pp. 848–853.
11. M. B. El-Arini, R. S. Conker, T. W. Albertson, J. K. Reagan, J. A. Klobuchar, and P. H. Doherty, "Comparison of real-time ionospheric algorithms for a GPS wide-area augmentation system (WAAS)," J. Navig.,vol. 44, no. 4, pp. 203–223, 1994–1995.

ISSN PRINT 2319 1775 Online 2320 7876

Research paper UGC CARE Listed (Group -I) Journal Volume 10, Iss 3, 2021

12. Saikumar, K. (2020). RajeshV. Coronary blockage of artery for Heart diagnosis with DT Artificial Intelligence Algorithm. Int J Res Pharma Sci, 11(1), 471-479.
13. Saikumar, K., Rajesh, V. (2020). A novel implementation heart diagnosis system based on random forest machine learning technique International Journal of Pharmaceutical Research 12, pp. 3904-3916.